New extended interpolating fields built from three-dimensional fermions

Francesco Scardino, Mauro Papinutto and Stefan Schaefer

University of Rome "La Sapienza", NIC DESY

Physical Features

- 3D propagators on initial and final time-slices grant better overlap with the states of interest thus leading to a better signal.
- Short distance behaviour greatly improved by the use of extended operators compared to standard local operators.
- Extended operators are well behaved under renormalization.
- 3D fermions mass $\tilde{m}$ tuned for a better overlap with physical states. Known how to keep $\tilde{m}$ fixed while the lattice spacing a is varied.

Baryonic Operators

Operators are representations of $O^{(a,b)}_{s,s_3} \in$ Spin$(3,\mathbb{Z})$ where (a,b) is the spin $SU(2)$ representation while s and s_3 are the total spin and its projection. The operators are written in the Weyl spinor formalism [3]:

Nucleon

$$\hat{p}^{(\frac{1}{2},0)}_{\frac{1}{2}\frac{1}{2}} = \frac{1}{2}(u_1 d_2 - u_2 d_1)u_1 \qquad \hat{p}^{(\frac{1}{2},0)}_{\frac{1}{2}-\frac{1}{2}} = \frac{1}{2}(u_1 d_2 - u_2 d_1)u_1$$

$$\tilde{p}^{(\frac{1}{2},0)}_{\frac{1}{2}\frac{1}{2}} = \frac{1}{2}(u_{\dot{1}} d_{\dot{2}} - u_{\dot{2}} d_{\dot{1}})u_1 \qquad \tilde{p}^{(\frac{1}{2},0)}_{\frac{1}{2}-\frac{1}{2}} = \frac{1}{2}(u_{\dot{1}} d_{\dot{2}} - u_{\dot{2}} d_{\dot{1}})u_1$$

$$p^{(\frac{1}{2},1)}_{\frac{1}{2}\frac{1}{2}} = \frac{1}{14}\{(u_{\dot{1}} d_{\dot{2}} + u_{\dot{2}} d_{\dot{1}})u_1 - 2u_{\dot{1}} d_{\dot{1}} u_2 + 2(u_{\dot{1}} d_2 - u_{\dot{2}} d_1)u_{\dot{1}}\}$$

$$p^{(\frac{1}{2},1)}_{\frac{1}{2}-\frac{1}{2}} = -\frac{1}{14}\{(u_{\dot{1}} d_{\dot{2}} + u_{\dot{2}} d_{\dot{1}})u_2 - 2u_{\dot{2}} d_{\dot{2}} u_1 + 2(u_{\dot{2}} d_1 - u_{\dot{1}} d_2)u_{\dot{2}}\}$$

Omega

$$\Omega^{(\frac{1}{2},1)}_{\frac{3}{2}\frac{3}{2}} = s_{\dot{1}} s_{\dot{1}} s_1 \qquad \Omega^{(\frac{1}{2},1)}_{\frac{3}{2}\frac{1}{2}} = \frac{1}{3}\{s_{\dot{1}} s_{\dot{1}} s_2 + s_{\dot{1}} s_{\dot{2}} s_1 + s_{\dot{2}} s_{\dot{1}} s_1\}$$

$$\Omega^{(\frac{1}{2},1)}_{\frac{3}{2}-\frac{3}{2}} = s_{\dot{2}} s_{\dot{2}} s_2 \qquad \Omega^{(\frac{1}{2},1)}_{\frac{3}{2}-\frac{1}{2}} = \frac{1}{3}\{s_{\dot{1}} s_{\dot{2}} s_1 + s_{\dot{2}} s_{\dot{2}} s_1 + s_{\dot{2}} s_{\dot{1}} s_2\}$$

$$\Omega^{(\frac{3}{2},0)}_{\frac{3}{2}\frac{3}{2}} = s_1 s_1 s_1 \qquad \Omega^{(\frac{3}{2},0)}_{\frac{3}{2}\frac{1}{2}} = \frac{1}{3}\{s_1 s_1 s_2 + s_1 s_2 s_1 + s_2 s_1 s_1\}$$

$$\Omega^{(\frac{3}{2},0)}_{\frac{3}{2}-\frac{3}{2}} = s_2 s_2 s_2 \qquad \Omega^{(\frac{3}{2},0)}_{\frac{3}{2}-\frac{1}{2}} = \frac{1}{3}\{s_1 s_2 s_2 + s_2 s_2 s_1 + s_2 s_1 s_2\}$$

These operators in the correlators have definite **parity**:

$$B^{\pm}_{(a,b)\oplus(b,a)} = B_{(a,b)} \mp B_{(b,a)}$$

Extended Operators

Non-local operators are built from quenched three dimensional fermions fields coupled via pseudo-scalar bilinears with ordinary four dimensional fermions in the four dimensional bulk.

The quark Propagator takes the form :

$$S(\mathbf{x},t,0) = \sum_{\mathbf{y},\mathbf{y}'} S_{3D}(\mathbf{x},\mathbf{y}'|x_0=t)\gamma_5 S_{4D}(t,\mathbf{y}';0,\mathbf{y})\gamma_5 S_{3D}(\mathbf{y};0|x_0=0)$$

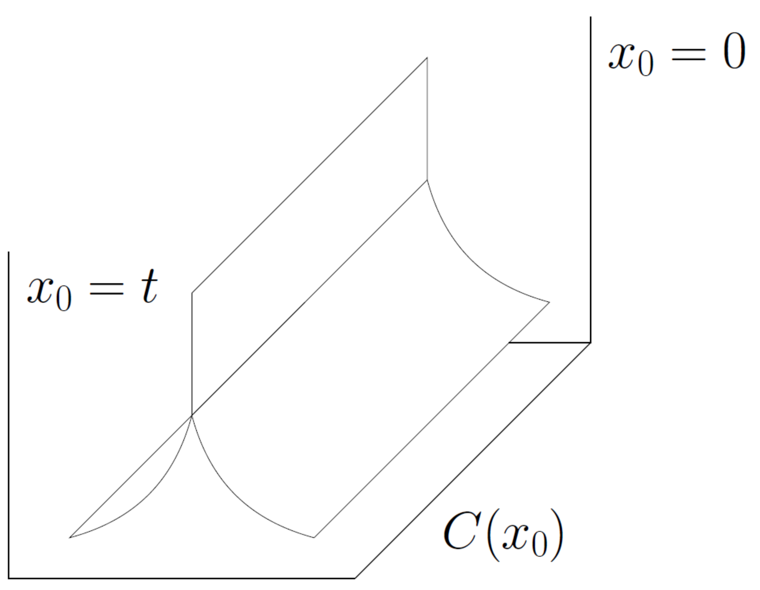

In this image there is a schematic representation of the baryonic two point function for the extended operators. On the time-slices $x_0 = 0$ and $x_0 = t$ there are the two 3D baryonic operators $\mathrm{B}^{\pm}$. Those are coupled via pseudo-scalar bilinear operators to the bulk and therefore can propagate between the time-slices.

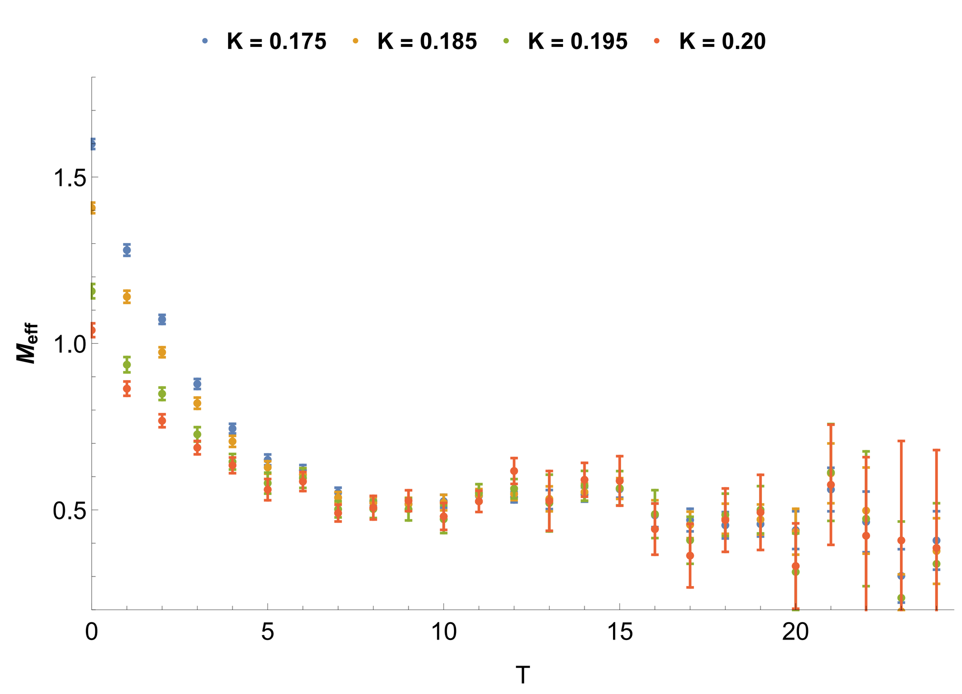

Fig. 1: Effective mass for different K_{3D}

Large K_{3D}, closer to the critical value $K^{crit}_{3D} = 0.208$ leads to a stronger suppression of excited states at the expense of computation time.Moreover the effective masses for greater K_{3D} are subject to greater fluctuations. We use as a possible compromise $K_{3D} = 0.185$

Comparison with other Methods

Data has been obtained from 2+1 $SU(3)$ degenerate **CLS** configurations [2] on a $96 \times 32 \times 32 \times 32$ lattice with open boundary conditions.

We compare with point sources:

$$\Psi_{pnt}(x,y) = \delta_{\alpha\beta}\delta(y-x)$$

and Jacobi smearing:

$$\Psi_{sm} = \sum_{i=0}^{N_{sm}} (k_{sm}\Delta)^i \, \delta_{\alpha\beta}\delta(y-x)$$

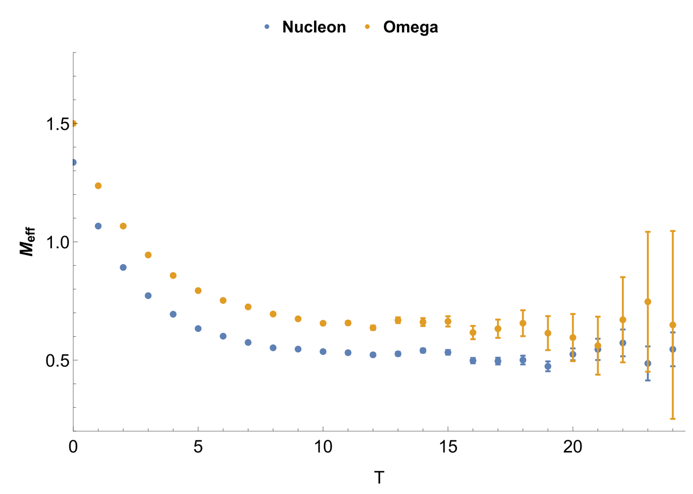

(a) Nucleon and Omega effective mass

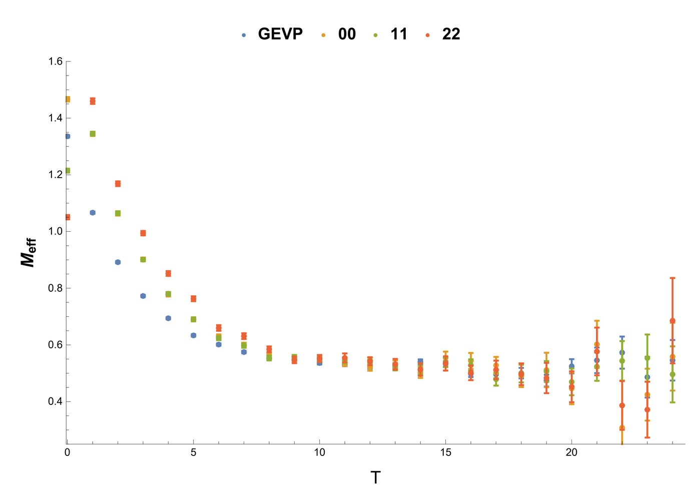

(b) Comparison between GEVP and single Nucleon Operators

In (a) is shown the effective mass of the Omega and the Nucleon obtained with the GEVP method, the extracted effective masses for the extended operators in lattice units are:

$$am_N = 0.526 \pm 0.002$$
$$am_\Omega = 0.649 \pm 0.003$$

In figure (b) a comparison between the effective mass extracted from the diagonal part of the correlator made by the single operators

$$C_{ii}(t) = \langle O_i O_i \rangle \qquad i = 0, \ldots, N-1$$

of the nucleon and the GEVP is made. The GEVP uses additional information by building a matrix correlation M_{ij} function from the N different interpolating operators on two different time-slices [1]. We have utilized the operators O_i and diagonalized M_{ij} for all methods separately :

$$M_{ij} = C^{-\frac{1}{2}}_{ik}(t_0) C_{kl}(t) C^{-\frac{1}{2}}_{lj}(t_0) \qquad i,j = 0, \ldots, N-1$$

Even with a small basis of operators, $N = 3$ for the nucleon and $N = 2$ for the omega, the GEVP has a better excited states suppression. Notice that the first two nucleon operators $i = 0$ and $i = 1$ in (b) have the same coupling with the nucleon state.

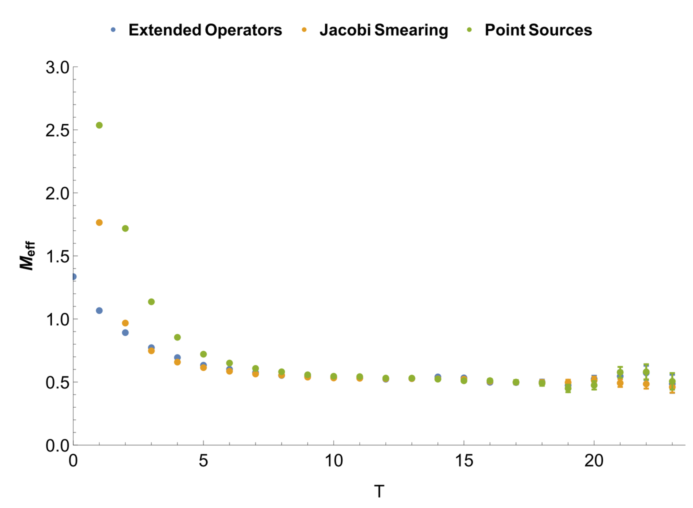

(c) Nucleon's effective masses

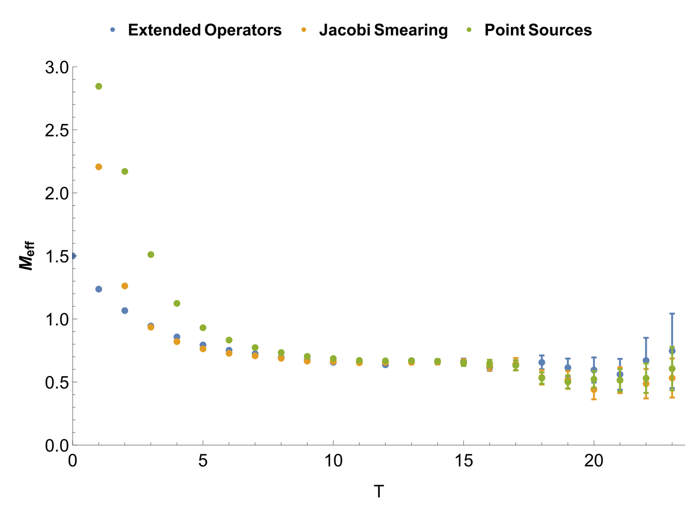

(d) Omegas's effective masses

In figure (c) and (d) a comparison between the three methods is made. It is possible to see that the extended operators have a better suppression of the contributions from the excited states as the short distance behaviour is much more regular.

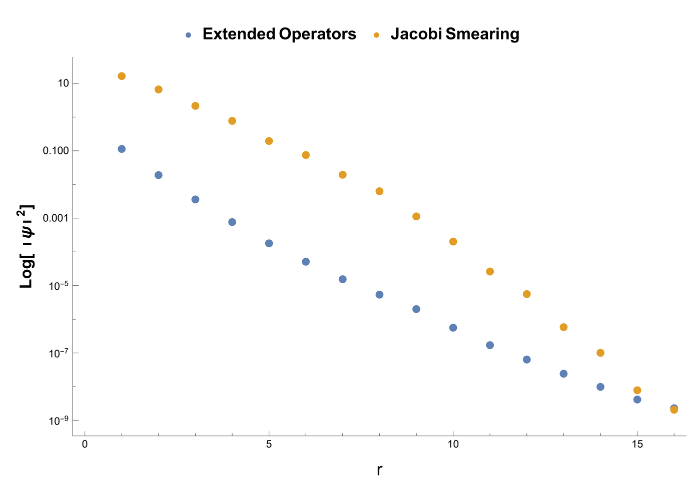

(e) 3D Source $|\psi|^2(r)$ as a function of distance

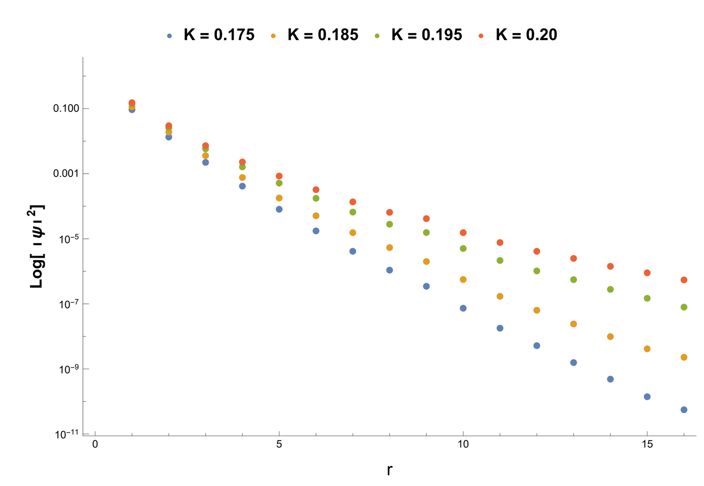

(f) $|\psi|^2$ at different K_{3D}

In figure (e) is plotted in log-scale the modulus squared of the 3D source as a function of distance for the extended operators and the Jacobi smearing. $|\psi|^2$ is rotationally invariant in both cases. In figure (f) $|\psi|^2$ is plotted at different K_{3D}. For $K_{3D} \to K^{crit}_{3D}$ the overlap increases.

References

[1] Martin Luscher and Ulli Wolff. How to Calculate the Elastic Scattering Matrix in Two-dimensional Quantum Field Theories by Numerical Simulation. *Nucl. Phys.*, B339:222–252, 1990.

[2] M. Bruno *et al.*, JHEP **1502**, 043 (2015) doi:10.1007/JHEP02(2015)043 [arXiv:1411.3982 [hep-lat]].

[3] Mauro Papinutto. Notes on baryon two-point correlators. *unpublished notes*, 2013.